JOURNAL OF VIROLOGY, May 1993, p. 2787–2798
0022-538X/93/052787-12$02.00/0

Vol. 67, No. 5

Assembly-Defective Point Mutants of the Human Immunodeficiency Virus Type 1 Gag Precursor Phenotypically Expressed in Recombinant Baculovirus-Infected Cells

SAW SEE HONG AND PIERRE BOULANGER*

Laboratoire de Virologie & Pathogénèse Moléculaires, CNRS, URA 1487, Institut de Biologie, Faculté de Médecine, 34060 Montpellier, France

Received 5 August 1992/Accepted 27 January 1993

Two substitution mutants of the human immunodeficiency virus type 1 *gag* gene product were isolated after nitrous acid mutagenesis of a recombinant baculovirus expressing a non-N-myristylated, p6-deleted Gag precursor (Pr49). Both mutants failed to assemble intracellular Gag virus-like particles, as does the parental recombinant, and therefore expressed a self-assembly defective (Sad) phenotype in insect cells. The mutations consisted of nonconservative changes involving highly conserved hydrophobic residues in the p24 domain, Leu to Pro at position 268 (L268P) and Leu to Ser at amino acid 322 (L322S). Experimental data suggested that the two mutated residues belonged to functionally different regions of the Gag precursor. (i) A partial complementation effect between the two mutants for Gag precursor assembly was observed in coinfection experiments. (ii) The two mutations showed different phenotypes when placed in the N-myristylated context, of which only the L268P mutation abolished extracellular budding and release of Gag particles at the plasma membrane. Both L268P and L322S mutants had a *trans*-dominant negative effect on the intracellular assembly of a non-N-myristylated, full-length (Pr55) Gag precursor expressed by a coinfecting recombinant. None of the mutants, however, showed any detectable effect in *trans* on membrane targeting and budding of the coexpressed N-myristylated wild-type Gag precursor.

The virion of human immunodeficiency virus type 1 (HIV-1) consists of a membrane-enveloped, nucleoprotein core containing the genomic RNA and nucleocapsid (NC) protein ($p15^{gag}$) surrounded by capsid (CA) proteins ($p24^{gag}$). The $p24^{gag}$ protein originates from the specific cleavage of a 55,000-Da polyprotein precursor (Gag Pr55) by the virus-coded protease (reviewed in references 2, 5, and 31). About 1,200 copies of p24 have been estimated to compose the capsid shell (13). Cleavage by the viral protease also generates additional structural proteins, the p17 matrix (MA) protein, which underlies the viral envelope, and the internal p15 NC protein, subsequently cleaved into p9 and p6 (15). Recent studies have shown that Gag precursors of HIV-1, simian immunodeficiency virus, and bovine immunodeficiency-like virus are capable of self-assembling into virus-like particles (VLP) within recombinant baculovirus-infected cells (4, 6, 19–21, 25).

We have previously described a baculovirus recombinant (AcNPVGag170 [25, 26]) which expresses a non-N-myristylated Gag precursor, amino-terminally fused to the first 8 amino acids of the polyhedrin sequence, and lacking the whole p6 domain and the last 11 amino acids from p9 (Pr49Δmyr). Its high efficiency in intracellular VLP formation suggested that the C-terminal domain p6 was dispensable for Gag precursor assembly (25, 26). Further deletion of the p9 domain, which generates a $Pr41^{gag}$ gene product, was found to be deleterious to the formation of intracytoplasmic VLP (6, 7, 25), but the effect of the p15 deletion could be partially compensated for assembly by the presence of a membrane-targeting myristyl residue at the N terminus of Gag (25, 26). Refined deletion mapping at the C terminus of the Gag precursor has localized the boundary for VLP formation to between amino acids 372 and 379, a region which overlaps the downstream cleavage site for HIV protease (9).

One can predict the existence of at least two types of domains in the Gag precursor molecule which are critical for assembly: (i) interacting sites which serve to establish contacts between Gag polyproteins and are directly involved in assembly and (ii) auxiliary domains, which indirectly participate in assembly by modifying the Gag conformation at (or in the vicinity of) the contact sites. Thus far, no direct clue for the localization and characterization of such critical domains in Gag precursor self-assembly are available. Since site-directed mutagenesis would imply some preconceived ideas on the polypeptide domains involved, random mutagenesis was preferred in the present study. Gag mutants were expressed in recombinant baculovirus-infected insect cells and screened for intracellular assembly of Gag precursor by immunofluorescence (IF) and electron microscopy (EM).

Two point mutants of the AcNPVGag170 recombinant, clones Gag48 and Gag49, which were found to express the self-assembly defective (Sad) phenotype, were thus isolated and characterized genotypically. Both mutations were mapped to the carboxy-terminal moiety of the p24 domain, a region which could correspond to one of the three assembly domains previously identified in the Rous sarcoma virus Gag precursor (31). Our observations that (i) some degree of complementation for the intracellular Gag assembly function occurred between the two Sad mutants and that (ii) different phenotypes were shown by the two mutations when they were reinserted into the N-myristylated, full-length Gag precursor Pr55 suggested that the mutated residues be-

* Corresponding author.

longed to topologically and/or functionally different subdomains of the HIV-1 Gag precursor.

MATERIALS AND METHODS

Virus and cells. The *Autographa californica* nuclear polyhedrosis virus (AcNPV)–HIV-1^{gag} recombinants used in this study were Gag170, Gag10, and Gag12myr, the construction and phenotypic properties of which have previously been described (25, 26). Briefly, Gag10 expresses a non-N-myristylated (Δmyr) and Gag12myr expresses an N-myristylated (myr), wild-type form of full-length Gag precursor (Pr55). Gag170 expresses a p6-deleted Gag precursor of 49 kDa (Pr49), amino-terminally fused to the N-terminal eight amino acids of the polyhedrin sequence. The recombinant Gag polyproteins were produced in *Spodoptera frugiperda* (Sf9) cells maintained in Grace's medium supplemented with 10% fetal calf serum. Recombinants PR107 and PR77 contain a synthetic gene for an active form and a carboxy-terminally deleted, inactive form of the HIV-1 protease (29), respectively, both expressed under the control of the polyhedrin promoter.

Mutagenesis of Gag170 recombinant. Nitrous acid mutagenesis was carried out on the Gag170 recombinant, following a procedure already described (14). Essentially, a purified virus stock of Gag170 (100 μl) with a titer of 10^8 PFU/ml was diluted with 900 μl of 0.7 M $NaNO_2$ in 1 M sodium acetate buffer, pH 4.6, and the reaction was allowed to proceed for 8 min at room temperature. The reaction was stopped by the addition of four volumes of 1 M Tris-HCl, pH 7.9, maintained at 4°C. The mixture was further diluted twenty times with Grace's Antheraea medium before plating out for plaque isolation. The plaques which formed were removed with Pasteur pipettes and resuspended in 0.5 ml of culture medium. These surviving viral clones were amplified in Sf9 cells and kept at 4°C as viral mutant stocks.

Coinfection experiments. Sf9 cells were infected simultaneously with the two Sad mutants, or with one of the Sad mutants and another AcNPV recombinant, at a total input multiplicity of infection (MOI) of 50 PFU per cell, 25 PFU of each unless otherwise mentioned. For EM, the cells were harvested and examined at 48 h postinfection (p.i.). For biochemical analyses of Gag10 + Sad mutant coinfections, cells were coinfected with a constant MOI of Gag10 (25 PFU per cell) and 0, 5, 15, and 25 PFU of Sad mutant per cell, respectively, and cells were harvested at 18, 24, and 40 h p.i. In protease susceptibility assays of Gag precursor in vivo, Sf9 cells were coinfected with a constant MOI of Sad mutant (25 PFU per cell) and variable MOI of the HIV-1 protease-expressing recombinants PR107 or PR77 (at 0, 5, 10, and 15 PFU per cell), and cells were harvested at 30 h p.i. Gag precursor cleavage was assayed by sodium dodecyl sulfate-polyacrylamide gel electrophoresis (SDS-PAGE) and immunoblot analysis (26).

IF. Sf9 cells were grown as monolayers on glass coverslips and infected at a MOI of 10 PFU per cell. At 24 h p.i., the cells were rinsed gently with phosphate-buffered saline (PBS) and fixed with methanol at −20°C. The cells were treated with 0.1% Triton X-100 in PBS for 5 min before incubating with mouse monoclonal antibody (MAb) against HIV-1 core antigen (anti-Pr55-p24, Epiclone #5001; Epitope, Beaverton, Oreg.) followed by the fluorescein isothiocyanate-conjugated second antibody. The cells were observed by using an Olympus BH2 microscope.

Electron and immunoelectron microscopy. Sf9 cells were infected at a MOI of 25 PFU per cell and harvested for EM processing at 48 h p.i. The cell pellets were fixed with 2.5% glutaraldehyde in 0.1 M phosphate buffer, pH 7.5, postfixed with osmium tetroxide (2% in H_2O), and treated with tannic acid (0.5% in H_2O). After dehydration, the specimens were embedded in Epon (Epon-812; Fulham, Latham, N.Y.). Sections were stained with 2.6% alkaline lead citrate–0.5% uranyl acetate in 50% ethanol. For immunogold staining (IGS), the cell specimens were embedded in metacrylic resin (Lowicryl K4M; Chemische Werke Lowi). An IGS reaction was carried out by successive reactions of cell sections with primary anti-Gag MAb (Epiclone #5001) at a dilution of 10 μg/ml in Tris-buffered saline, overnight at 4°C, and 5-nm colloidal gold-labeled anti-mouse immunoglobin G antibody for 1 h at room temperature (EM-GAM5; BioCell Research Lab). Specimens were poststained with 0.5% uranyl acetate and examined under a Philips EM-300 electron microscope.

Electrophoretic and immunological analyses. Protein samples were electrophoresed in SDS–12% polyacrylamide gels (SDS-PAGE; ratio of acrylamide to bisacrylamide of 50:0.8), with a discontinuous buffer system (11). The proteins were electrically transferred from SDS gels onto nitrocellulose membranes (ECL; Amersham) at 180 mA for 90 min, using a semi-dry system (Cambridge Electrophoresis, Ltd, Cambridge, United Kingdom). After saturation in 5% skim milk in TNT buffer (20 mM Tris-HCl [pH 7.5], 150 mM NaCl, 0.05% Tween 20) for 1 h at room temperature, the Gag proteins were detected on blots by successive reactions with (i) a mixture (1:1, vol/vol) of MAb directed against Pr55-p24 (Epiclone #5001) and p17 (Epiclone #5002) at a dilution of 1:1,000 each in TNT buffer for 16 h at room temperature; (ii) alkaline phosphatase-labeled anti-mouse immunoglobulin G conjugate (Sigma); and (iii) nitroblue tetrazolium–5-bromo-4-chloro-3 indolyl phosphate toluidinium (NBT-BCIP) cosubstrate-substrate (Boehringer) for color development. The Gag precursor concentrations in cell culture media and cytoplasmic extracts were determined by antigen capture enzyme-linked immunosorbent assay (ELISA), using two different anti-p24 MAb (27), and bacterially expressed, chromatographically purified p24 (Transgene, Strasbourg, France) as the standard. Peptide fingerprinting was performed in SDS-PAGE (3), with endoproteinase Glu-C (Boehringer) and chymotrypsin (Sigma).

Quantitative assays for Gag precursor self-assembly. Four different methods of Gag precursor self-assembly were tested: (i) separation of assembled Gag particles from soluble Gag polyproteins by ultracentrifugation analysis of cell lysates (22); (ii) analysis of Gag monomeric and polymeric forms by nondenaturing SDS-PAGE (NDS-PAGE) (17, 18); (iii) reversible cross-linking of assembled Gag in cell lysates using two cleavable diimidoesters (Pierce), 3,3′-dithio-bis-(propionic acid *N*-hydroxysuccinimide ester), and dimethyl 3,3′-dithio-bis(propionimidate) dihydrochloride; and (iv) immunoelectron microscopy. The first three approaches failed to give a reproducible quantitative picture of the number of Gag particles assembled in vivo. Probably because of the lack of solubility of assembled Gag protein edifices or to interactions with cytoskeletal elements, significant amounts of Gag precursor were found to be pelleted at every centrifugation step of the cellular fractionation. On the other hand, Gag oligomers possibly existing in cell extracts seemed not to resist the presence of SDS in the gel buffer of the NDS-PAGE technique, and chemical cross-linking did not show any prominent Gag precursor oligomer species of higher order than a discrete band of Gag precursor dimers (unpublished data).

The intracellular self-assembly of Gag into VLP was

therefore quantitatively assayed by EM analysis of recombinant-infected cell sections. The number of VLP per surface unit of cytoplasm and nucleoplasm gave first a crude estimate of the self-assembling capacity of Gag precursors within cell compartments. Quantification was then performed after IGS of cell sections. Colloidal gold grains found associated with VLP or free within the cytoplasm and the nucleoplasm were counted per square micrometer of cell section. The efficiency of the Gag assembly process was estimated from the ratio of bound VLP to the total number of grains. A minimum number of 1,000 grains were counted per section of whole cell, on five different electron micrographs, and the background for nonspecific immunogold labeling of AcNPV wild-type infected cells was subtracted (18, 25).

Epitope analysis of Sad mutations. A panel of 18 MAb directed against HIV-1 Gag precursor (24) was used for epitope analysis of the Gag48 and Gag49 mutants. The target epitopes of these MAb have been mapped in competition assays with synthetic peptides overlapping portions of the Gag polyprotein sequence between amino acids 11 and 320 (24). Preparative SDS gels were loaded with equivalent amounts of Gag polyprotein from Gag170-, Gag48-, and Gag49-infected cell lysates. The proteins in the gels were electrically transferred onto nitrocellulose membranes which were subsequently cut into strips for reaction with each of the MAb.

DNA sequencing. The HIV-1 *gag* genes from the baculovirus recombinants Gag170, Gag48, and Gag49 were isolated and cloned into the pUC18 vector. Three fragments, spanning the whole *gag* gene (30) and flanking sequences from the baculoviral polyhedrin, were subcloned into the *Hin*dIII site or between the *Hin*dIII and *Kpn*I or *Hin*dIII and *Sma*I sites of pUC18: (i) the *Eco*RV-*Hin*dIII fragment contained the N-terminal portion of the *gag* gene and the polyhedrin promoter sequence, (ii) the *Hin*dIII-*Hin*dIII fragment corresponded to the central fragment of *gag*, and (iii) the *Hin*dIII-*Kpn*I fragment comprised the C-terminal extremity of p24, most of the p9 sequence (from Ser-310 to Ile-437), and the polyhedrin polyadenylation signal (25). The central fragment of 637 bp was inserted in both orientations. The parental and mutant fragments were sequenced six times in both orientations in an automatic DNA sequencer (373A DNA Sequencer; Applied Biosystems), using the 18-mer sequencing forward and reverse (−21M13) primers, and the *Taq* Dye-Primer cycle sequencing kit (Applied Biosystems). The *Taq* polymerase was purchased from Cetus Corporation. The sequence data were then analyzed with the aid of 373A Macintosh-based software (8). Nucleotide sequences were then controlled by manual sequencing. The *Hin*dIII-*Hin*dIII central fragment was cleaved at its unique *Pst*I site, and the *Hin*dIII-*Kpn*I 3′-end fragment was cleaved at its unique *Apa*I site. The resulting fragments were subcloned into pBluescript II KS(−) and sequenced (10) with a ^{35}S-T7 sequencing kit (Pharmacia).

RESULTS

Isolation of mutants defective in intracellular self-assembly of Gag precursor (Sad phenotype). The baculovirus recombinant Gag170, which expresses a p6-deleted Gag precursor fused to the polyhedrin-derived MPDYSYRP octapeptide at its N terminus (Pr49Δmyr [26]), was selected as the parental recombinant for random mutagenesis of the *gag* gene. (i) Deletion of the p6 domain has been shown to result in a minimal nuclear localization of Gag precursors and a high level of intracytoplasmic assembly (25). (ii) The N-terminal sequence detectable with anti-polyhedrin antibodies could advantageously be used as an epitope tag to identify the Gag precursor species within particles and also to map processing sites. Mutagenesis by NO_2H of a Gag170 parental viral stock resulted in the loss of about 2 $\log_{10}$ units in final infectivity of the recombinant baculovirus suspension, as estimated by plaque assay. Seventy-four NO_2H-surviving clones were thus isolated and amplified. Immunoblot analysis of lysates from cells infected with the surviving clones showed that 26 of them still expressed the *gag* gene at parental-type levels (not shown). These clones were retained as potential *gag* mutants and further characterized, while the others, which were possibly altered in some viral functions involved in the level of *gag* expression, were discarded.

Cells infected with each of the 26 isolated clones were then analyzed by IF, using anti-Pr55-p24 MAb, and the fluorescent staining reaction was compared with the parental pattern. Three types of IF patterns were observed: (i) a reticulate cytoplasmic fluorescence, characteristic of the parental Gag170-infected cells; (ii) a diffuse cytoplasmic fluorescence, observed with clone Gag48; and (iii) a speckled perinuclear fluorescence, as obtained with clone Gag49 (data not shown). From the IF data, it appeared that two clones, Gag48 and Gag49, were good candidates for being mutated in a function required for intracytoplasmic Gag assembly. This hypothesis was confirmed by EM analysis of cells harvested at 48 h p.i. In contrast to the abundance of cytoplasmic VLP shown by parental Gag170 (3 to 4 VLP per μm^2), VLP were found in low numbers in very few cells with Gag48 (less than 0.5 VLP per μm^2) and none were detected with Gag49 (Fig. 1).

The Gag self-assembly process in vivo was assayed by quantitative immunoelectron microscopy, using IGS of recombinant-infected cell sections reacted with anti-Gag antibody. Its efficiency was estimated by the ratio of gold grains bound to VLP versus total gold grains (free plus bound) counted per unit surface area of cytoplasm or nucleoplasm. For the cytoplasm, the ratio was found to be higher than 60% for parental Gag170 and less than 5 and 0.01% for Gag48 and Gag49, respectively (Table 1). In the nucleus, Gag particles were found in scarce amounts with parental Gag170 (0.2 VLP per μm^2), with an intranuclear assembly efficiency of 7% (Table 2), and rarely or never observed with Gag48 or Gag49. Thus Gag48 and Gag49 appeared to be phenotypically defective in self-assembly of Gag precursors within both cytoplasmic and nuclear compartments.

Genotype of the Sad mutants. DNA sequence analysis of the *Eco*RV-*Hin*dIII fragment isolated from the two Sad mutant DNAs, which contains the N-terminal portion of the *gag* gene and a baculovirus DNA sequence of 93 nucleotides upstream of the polyhedrin ATG start codon, indicated that there was no mutation in the polyhedrin promoter. Sequencing of the *Hin*dIII-*Kpn*I fragment showed no mutation in the out-of-phase portion of the polyhedrin gene downstream to the cloning site or in its polyadenylation signal. Single mutations were found in the *gag* genes of Gag48 and Gag49, both located in the p24 domain. Gag48 showed a CTG-to-CCG mutation at codon 268, implying a NO_2H-induced A-to-I transition of the second base of the triplet on the *gag* noncoding strand in the recombinant baculovirus genome, which changed the leucine 268 to a proline (L268P). The mutation in Gag49 consisted of a leucine-to-serine mutation at codon 322 (L322S), with a TTG-to-TCG change on the *gag* coding strand, resulting from the same mechanism described above. The replacement of a leucine residue (a hydrophobic, bulky amino acid) by a proline, which bends the polypeptide

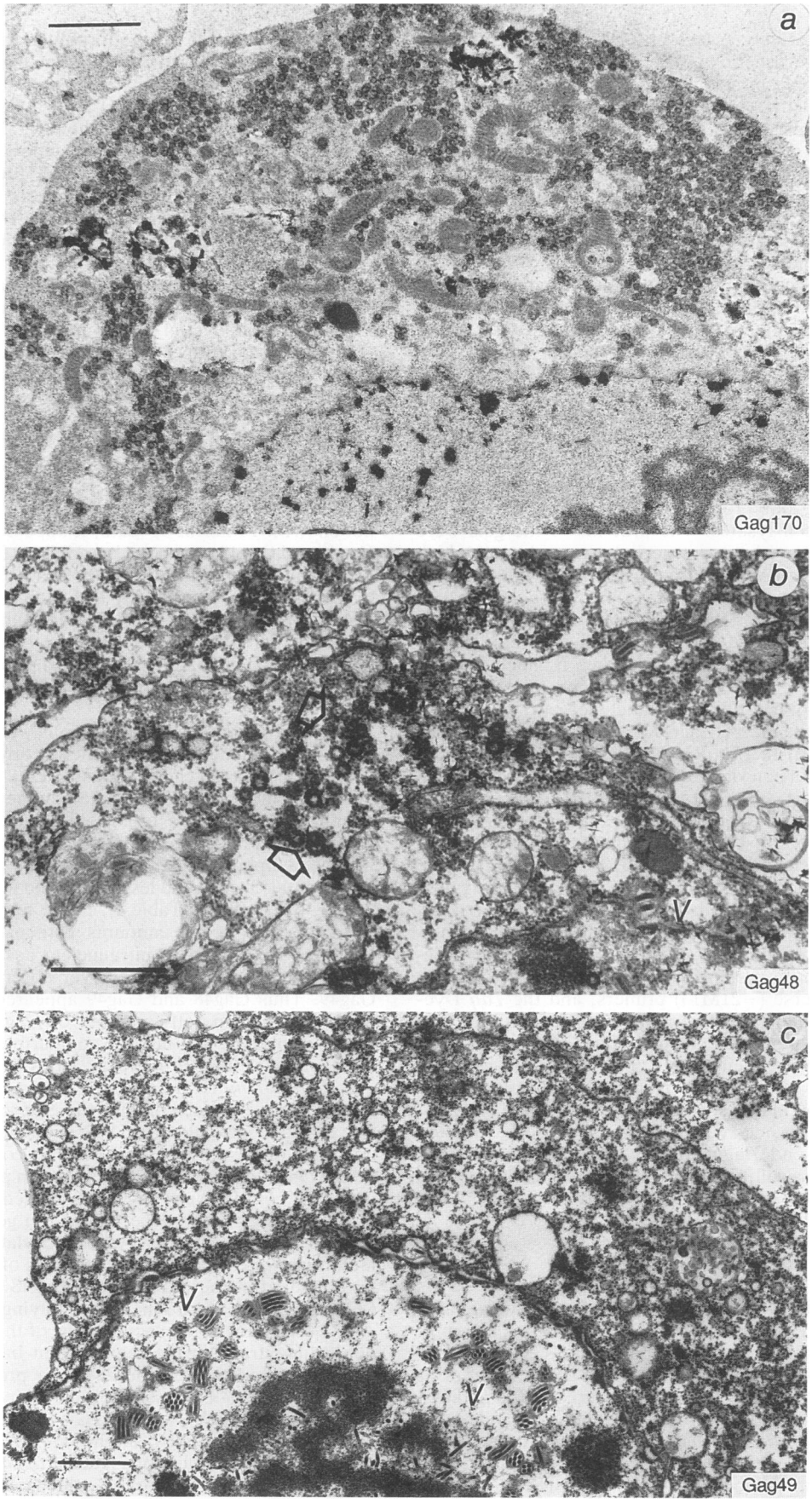
a
Gag170
b
V
Gag48
c
V
V
Gag49

TABLE 1. Efficiency of intracytoplasmic Gag precursor assembly in parental recombinant- and Sad mutant-infected cells[a]

Recombinant	No. of grains/μm²			Assembly efficiency[b]
	Particle bound	Free	Total	
Single infections				
Gag170 (parental)	39.9 ± 2.7	22.0 ± 5.1	61.9	64.4
Gag48(L268P)	1.9 ± 0.4	42.7 ± 6.2	44.6	4.3
Gag49(L322S)	≤0.1	53.9 ± 8.2	54.0	≤0.01
Gag10(Pr55Δmyr)[c]	15.3 ± 4.8	3.4 ± 1.0	18.7	81.8
Coinfections				
Gag48 + Gag49	6.5 ± 4.6	20.3 ± 2.6	26.8	24.2
Gag170 + Gag48	11.2 ± 4.7	33.7 ± 2.0	44.9	24.9
Gag170 + Gag49	8.3 ± 2.8	35.5 ± 3.9	43.8	18.9
Gag10 + Gag48	4.3 ± 1.1	33.3 ± 8.3	37.6	11.4
Gag10 + Gag49	1.7 ± 1.0	37.0 ± 11.5	38.7	4.3

[a] The intracytoplasmic self-assembly of Gag precursors into VLP was quantitatively analyzed by IGS of recombinant-infected cell sections reacted with anti-Pr55-p24 MAb. Figures in the table represent the number of 5-nm colloidal gold grains per square micrometer (± standard deviation) which were found associated with VLP or free within the cytoplasm. A minimum number of 1,000 grains were counted per cell, on five different electron micrographs of cell sections (18, 25).

[b] The efficiency of intracytoplasmic Gag precursors assembly was estimated from the ratio of VLP-associated grains to the total number (bound plus free) of grains counted per square micrometer of surface of cytoplasm, expressed as percentage of the total.

[c] Gag10 expresses a non-N-myristylated, full-length Gag precursor (Pr55Δmyr).

TABLE 2. Nuclear localization and intranuclear assembly efficiency of Gag precursors in parental recombinant- and Sad mutant-infected cells[a]

Recombinant	Nuclear transport[b]	No. of grains/μm²		Assembly efficiency[c]
		Particle bound	Free	
Single infections				
Gag170 (parental)	0.14	0.6 ± 0.2	8.2 ± 1.8	7.0
Gag48(L268P)	0.14	≤0.01	6.3 ± 2.9	0.0
Gag49(L322S)	0.13	≤0.01	7.3 ± 2.3	0.0
Gag10(Pr55Δmyr)	2.07	34.6 ± 9.3	4.1 ± 0.3	89.4
Coinfections				
Gag48 + Gag49	0.57	3.7 ± 1.9	17.9 ± 1.2	17.1
Gag170 + Gag48	0.77	0.15 ± 0.06	34.6 ± 6.4	0.004
Gag170 + Gag49	0.25	0.12 ± 0.03	10.9 ± 1.1	0.01
Gag10 + Gag48	1.85	10.4 ± 4.9	59.4 ± 16.1	14.9
Gag10 + Gag49	1.00	7.8 ± 3.7	30.3 ± 12.6	20.4

[a] Figures in the table represent the number of free or VLP-associated colloidal gold grains per square micrometer (± standard deviation) of nucleoplasm of cell sections immunoreacted with anti-Pr55-p24 MAb and 5-nm colloidal gold-labeled conjugate.

[b] The efficiency of nuclear transport of Gag precursor was estimated from the ratio of the total number of nuclear to the total number of cytoplasmic gold grains per square micrometer of cell section.

[c] The efficiency of intranuclear Gag precursor assembly was estimated from the ratio of VLP-associated to the total number of gold grains counted per square micrometer of surface of nucleoplasm, expressed as percentage of the total.

backbone, or by a serine, which is considered a small polar neutral residue, represents a nonconservative mutation.

Extracellular release of nonparticulate form of Sad mutant Gag precursors. N-Myristylated and non-N-myristylated Gag precursors have been shown to be released as soluble Gag polyproteins into the culture medium of recombinant-infected insect cells, via a mechanism which is apparently independent of budding and is also not due to cell lysis (26). The levels of expression and secretion of Sad mutant Gag precursors were qualitatively estimated by SDS-PAGE and immunoblotting analysis and then quantitatively assayed by antigen capture ELISA of cytoplasmic extracts and culture medium samples from recombinant-infected cells. Similar levels of Gag precursor were released into the culture medium by Gag170-, Gag48-, and Gag49-infected cells. The extracellular Gag concentrations ranged between 10 and 20 μg/10⁶ cells (0.01 to 0.02 mg/ml of culture fluid) between 30 and 40 h after infection. Since intracellular Gag yields ranged between 12 and 15 μg of Gag per 10⁶ cells at 30 h and 25 and 30 μg of Gag per 10⁶ cells at 40 h (viz. 150 × 10⁶ to 200 × 10⁶ and 350 × 10⁶ to 400 × 10⁶ molecules per cell at 30 and 40 h after infection, respectively), the proportion of extracellular Gag represented 35 to 45% of the total Gag recovered for Gag48, Gag49, and parental Gag170. This value, which was not significantly different from the one previously reported for most of the non-N-myristylated Gag precursors (26), suggested that none of the mutations in Gag48 or Gag49 negatively affected the secretion of the nonparticulate form of non-N-myristylated-minus Gag precursor by insect cells.

Complementation analysis of Sad mutants and parental Gag170 in coinfection experiments. Coinfections of insect cells were carried out to analyze the possible rescue of the mutant Gag function by the sister mutant or parental recombinant or alternatively its dominance over the parental Gag. As shown in Table 1, some complementation effect for intracytoplasmic assembly of Gag precursor was observed in cells coinfected with the two mutants GagL268P (Gag48) and GagL322S (Gag49). The number of VLP per unit surface area of sectioned cell was three times higher in coinfected cells than in GagL268P single-infected cells, and the efficiency of cytoplasmic assembly was six times higher. The nuclear concentration of Gag precursor and its intranuclear assembly efficiency also increased significantly in GagL268P-GagL322S coinfected cells (Table 2). This suggested that the mutations in GagL268P and GagL322S involved two distinct assembly subdomains in the p24 sequence and that the defect in one mutant Gag precursor could be partially complemented by the corresponding sister mutant domain.

Such a compensatory effect did not occur at detectable levels with parental Gag170, and no significant degree of complementation could be observed in coinfected cells. Instead, the apparent efficiency of Gag precursor assembly decreased from 64% in cells infected with Gag170 alone to 25% in cells coinfected with Gag170 and GagL268P and to 19% with GagL322S (Table 1). The same negative effect on Gag precursor assembly was observed within the nucleus of coinfected cells (Table 2). However, no dominant effect seemed to be involved in coinfection of Sad mutants with

FIG. 1. Electron micrographs of Sf9 cells infected with parental recombinant Gag170 (a), Sad mutant Gag48(L268P) (b), and Sad mutant Gag49(L322S) (c). In panel a, VLP of 120 to 130 nm in diameter can be seen in numbers within the cytoplasm; in panel b a few VLP are seen in rare cells (arrows). Note that the absence of detectable VLP in panel c is not due to underinfection of the cells, as demonstrated by the abundance of baculovirions (V) within the nucleus. Bars, 1 μm.

parental Gag170, since the experimental values obtained were compatible with the juxtaposition of two forms of Gag precursors self-assembling with high (Gag170) and low (GagL268P and GagL322S) efficiencies in the same compartment.

Phenotype of the L268P and L322S mutations placed in the N-myristylated, full-length Gag precursor context. Since both L268P and L322S mutations showed a deleterious effect on the intracellular assembly of non-N-myristylated Gag precursors into core structures, it was important to further characterize these mutations in the N-myristylated context. L268P and L322S mutations were therefore reintroduced into an AcNPV recombinant expressing an N-myristylated, full-length Gag precursor (Pr55myr). They were referred to as Gag1248myr for the L268P and Gag1249myr for the L322S mutation, respectively. As previously shown (26), the N-myristylated wild-type Gag precursor released in the extracellular medium by Gag12myr-infected cells consists of (i) budded particles which sediment with an apparent coefficient of 600S and a density of 1.15 g/ml in sucrose gradient and (ii) nonparticulate, soluble Gag precursors which sediment as molecules of 3 to 7S.

The total amount of extracellular Gag precursor released by mutant Gag1248myr-infected cells was drastically reduced, as compared with wild-type Gag12myr. The levels of Gag precursor secretion ranged between 0.5 and 1.0 $\mu g/10^6$ Sf9 cells at 48 h p.i., as assayed by immunocapture ELISA (26), i.e., 25 to 60 times lower than that of wild-type Gag12myr (25 to 30 $\mu g/10^6$ cells). In immunoblotting analysis of velocity gradients, no Gag protein signal was detected in the fractions corresponding to 600S-sedimenting particles, and soluble Gag precursor was found in barely detectable concentrations in the top fractions (data not shown). When Gag1248myr-infected cells were analyzed by EM, no VLP budding was visible at the surface, but localization of electron-dense material, 20 to 22 nm in thickness, was observed along the inner face of the plasma membrane (Fig. 2a to c). All these data indicated that secretion of both particulate and nonparticulate forms of Gag precursor was almost totally abolished by the L268P mutation expressed in the N-myristylated context.

On the other hand, the L322S mutation provoked only slight changes in the secretion of N-myristylated Gag. Gag precursor was found at two- to fivefold-lower levels in Gag1249myr-infected cell culture fluids than in wild-type Gag12myr. Velocity gradient centrifugation analysis of cell culture supernatants and EM examination of Gag1249myr-infected cells showed a lower efficiency in VLP budding (Fig. 2d) compared with cells expressing the wild-type Gag precursor (Fig. 2f), and many budding particles presented an irregular shape (Fig. 2e).

When reintroduced into an N-myristylated, p6-deleted context, the L268P and L322S mutations showed the same phenotypes as their full-length Gag precursor counterparts, suggesting that the presence or absence of the carboxy-terminal p6 domain had little influence, if any, on the expression of these mutations (data not shown).

Effect in *trans* of the L268P and L322S mutations on the intracellular assembly of non-N-myristylated, full-length Gag precursor. Each Sad mutant was analyzed in coinfection with Gag10 (25), an $AcNPV^{gag}$ recombinant which expresses a non-N-myristylated form of full-length Gag precursor (Pr55Δmyr). Pr55Δmyr has been shown to form core structures within the cytoplasm and the nucleus of insect cells with a high efficiency (25) (Fig. 3a and Table 2). Cells were infected simultaneously by two recombinants at the same input MOI and then analyzed after 48 h under the electron microscope for the occurrence of intracytoplasmic and intranuclear Gag particles. As shown in Fig. 3b and c, the function of self-assembly of Gag cores appeared to be altered in the cytoplasm and nucleus of cells coexpressing Pr55Δmyr and a Sad mutant Gag precursor (GagL268P or GagL322S). Some Gag particles remained visible within the cytoplasm, in close vicinity to amorphous inclusions located at the perinuclear region. The efficiency of Gag precursor assembly decreased from 82% in single infections with Gag10 to 4 to 11% in coinfections within the cytoplasm (Table 1) and from about 90% to 15 to 20% within the nucleus (Table 2).

When compared to single Gag10-infected cells, the ratio of total (assembled plus free) nuclear to total cytoplasmic Gag precursor molecules was found to remain unchanged in Gag10-GagL268P coinfections (1.85) and to be twofold lower in the case of Gag10-GagL322S (1.0 [Table 2]). Considering that Gag precursors expressed by both GagL268P and GagL322S were mainly localized in the cytoplasm, whereas Gag10(Pr55Δmyr) was massively accumulated in the nucleus (Table 2, Fig. 3a, and reference 25), the theoretical ratio of nuclear to cytoplasmic Gag in coinfection experiments in which two Gag precursors would be expressed and transported independently would be around 1. This was the value precisely obtained with cells coinfected with Gag10 and GagL322S (Table 2). The value of 1.85 therefore implied that the nuclear transport of Gag was somehow facilitated in cells coexpressing Pr55Δmyr and GagL268P, whereas it was not modified in the case of Pr55Δmyr-GagL322S coexpression. The following experiments were designed to analyze the possible molecular interactions between Gag polyproteins coexpressed by the Sad mutants and parental Gag170 (Pr49Δmyr) or Gag10(Pr55Δmyr).

One of the advantages of the coinfection of cells with Gag10 and Sad mutants expressing a p6-deleted Gag precursor (such as parental Gag170) was that the different *gag* gene products could easily be distinguished by their apparent molecular masses, 55 and 49 kDa, respectively (26). Cells were simultaneously infected with a constant MOI of the recombinant virus expressing the reporter Gag precursor and with various MOI of the recombinant expressing the effector protein and were harvested at different times after infection. In the case of the coinfection with Gag10 and the Sad mutant, Pr55Δmyr was the reporter and the mutant Gag precursor was the effector, and any biological processing of the Pr55Δmyr reporter would be readily detected by SDS-PAGE and immunoblotting. As a control, cells were coinfected with Gag10 and the parental Gag170 at the same MOI ratios. As shown in Fig. 4, Pr55Δmyr was cleaved into major 52- and 51-kDa doublet bands by cellular enzymes in single-infected cells at late times after infection (24 to 40 h), a phenomenon already described (26). In coinfection with Gag170, the 52- and 51-kDa cleavage products were still visible (Fig. 4a). On the other hand, coinfection with GagL268P or GagL322S resulted in an interference with Pr55Δmyr proteolysis, which was observed even at low MOI of the coinfecting Sad mutant (5 to 15 PFU per cell). The 52- and 51-kDa products became barely visible for MOI ratios of 15 to 25, whereas the signal in the 55-kDa precursor band progressively increased with the time of coinfection (Fig. 4b and 4c). This result suggested that some interactions occurred between the Gag precursors expressed by Gag10 and GagL268P or GagL322S, which could prevent the proteolysis of Pr55Δmyr by host cell enzymes. These interactions would explain the electron-dense perinuclear inclusions visible under the electron microscope (Fig. 3b and c).

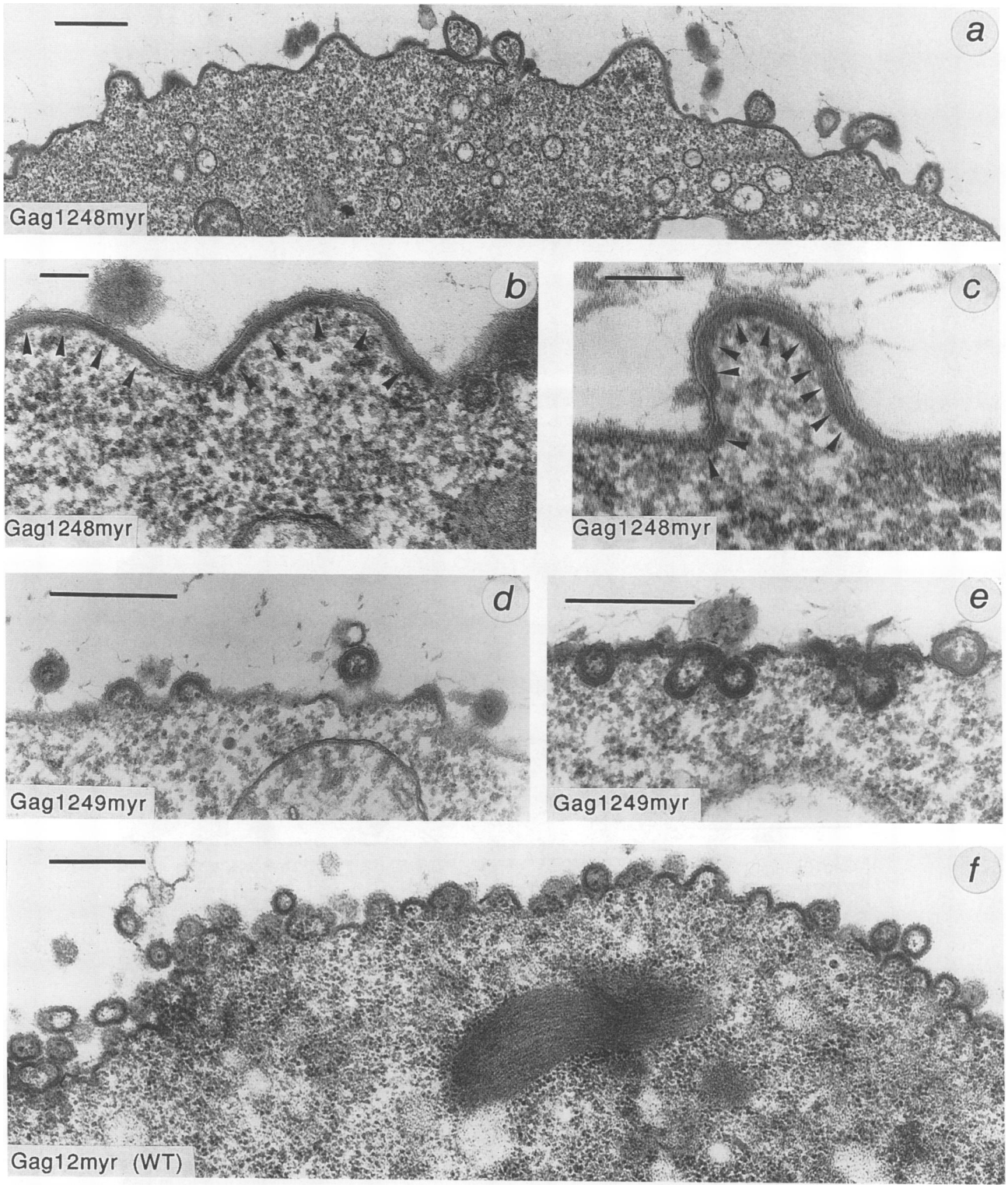

FIG. 2. Expression of the L268P (Gag1248myr) and L322S (Gag1249myr) mutations in an N-myristylated context. Sf9 cells were infected with Gag1248myr (a to c), Gag1249myr (d and e), or wild-type Gag12myr (f), and examined at 48 h p.i. Panels b and c show enlargements of portions of Gag1248myr-infected cell plasma membrane showing local accumulations of electron-dense material, 20 to 22 nm in thickness, at the inner face of the plasma membrane (arrowheads). In panel e, note the irregular shape of several Gag particles. Bar represents 1 μm in panel a, 100 nm in panels b and c, and 500 nm in panels d to f.

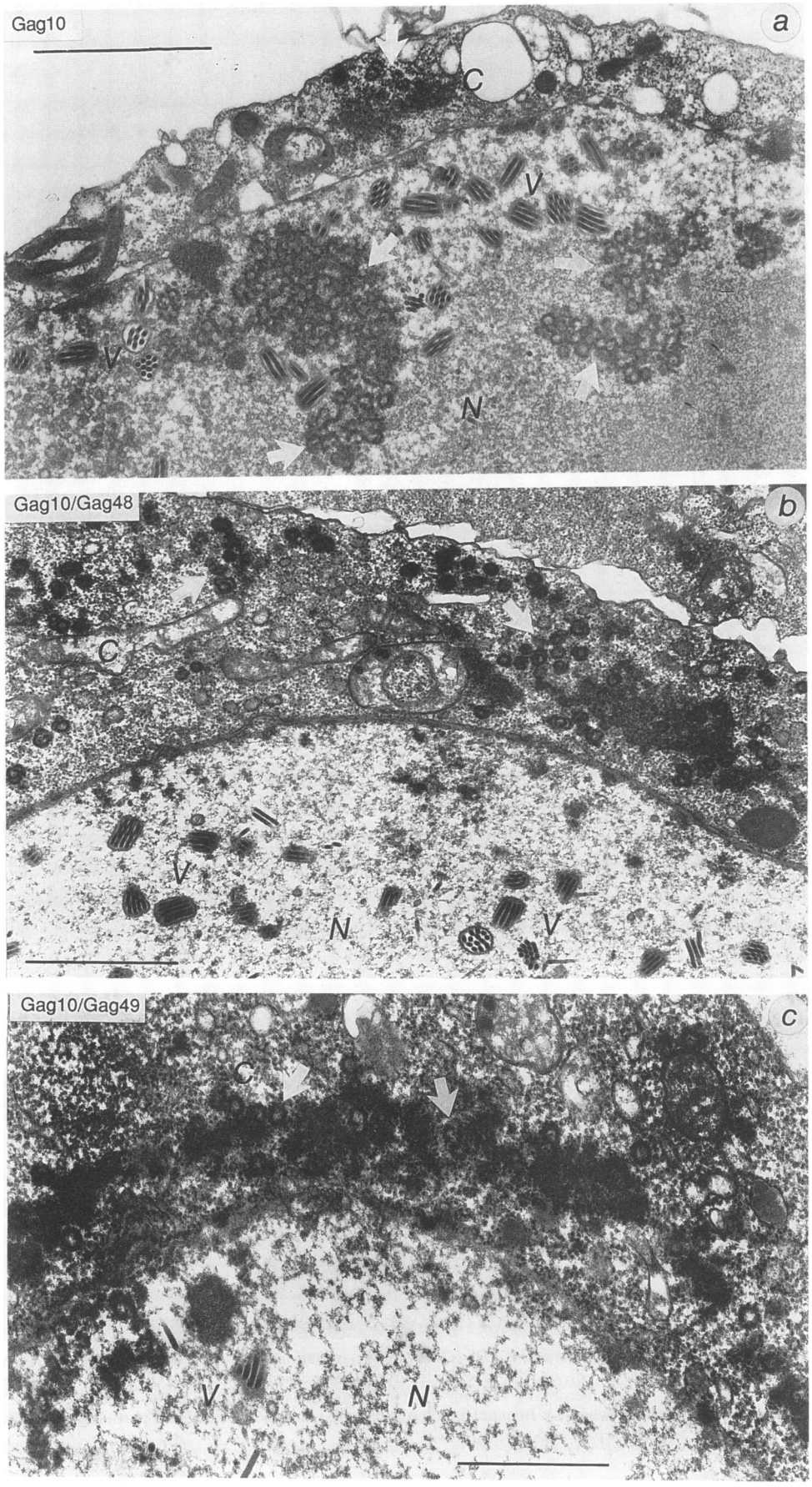
Gag10
a
C
V
V
N
Gag10/Gag48
b
C
V
N
V
Gag10/Gag49
c
C
V
N

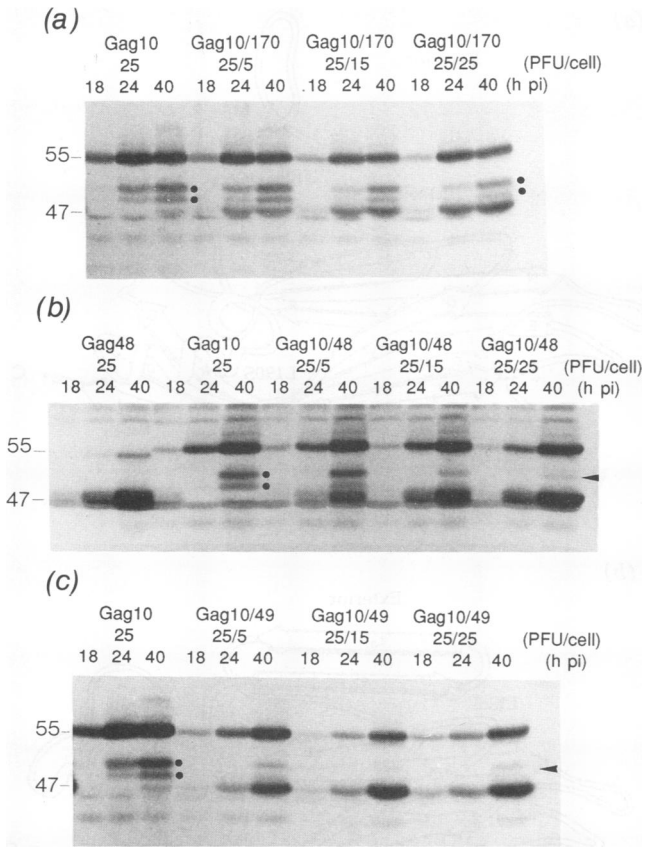

FIG. 4. Immunoblot analysis of HIV-1 Gag precursors expressed in cells coinfected with Gag10 and Gag170 (a), Gag10 and Gag48(L268P) (b), and Gag10 and Gag49(L322S) (c). Cells were infected at constant MOI for the reporter Gag (full-length Gag precursor Pr55Δmyr, expressed by Gag10) and at various MOI for the effector Gag (p6-deleted Gag precursor Pr49, expressed by Gag170, Gag48, or Gag49). Cell samples were harvested at 18, 24 and 40 h p.i., and cell lysates were analyzed by SDS-PAGE and immunoblotting with anti-Pr55-p24 MAb. Dots indicate the major Pr55Δmyr proteolytic products which decrease in intensity upon coinfection with Gag48 and Gag49 (arrowhead).

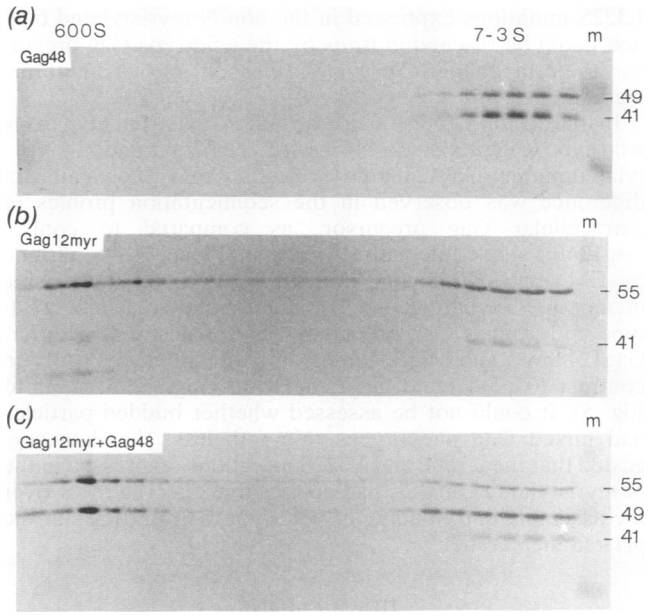

FIG. 5. Velocity gradient centrifugation analysis of extracellular Gag precursor, released from cells singly infected with Gag48 (L268P) (a) or Gag12myr (b) or coinfected with Gag12myr and Gag48(L268P) (c). Aliquots from the gradient fractions were analyzed by SDS-PAGE and immunoblotting with anti-Pr55-p24 MAb. Gag particles sediment at 600S, whereas nonparticulate, soluble Gag precursor molecules sediment at 3 to 7S (26). Lanes m, molecular mass markers. Figures on the right are apparent molecular masses expressed in kilodaltons. Not shown are culture supernatant analyses from cells singly infected with Gag170 or Gag49(L322S), which gave patterns similar to those in panel a, and from cells coinfected with Gag12myr and parental Gag170 or with Gag12myr and Gag49(L322S), which gave patterns similar to those in panel c.

Effect in *trans* of the L268P and L322S mutations on the extracellular release of N-myristylated Gag precursor. The possible effects in *trans* of the L268P and L322S mutations on the extracellular release of particulate and nonparticulate forms of wild-type Gag precursor were analyzed by coinfection experiments performed in two different situations. Wild-type Pr55myr (Gag12myr) was coexpressed with (i) non-N-myristylated Pr49 from the original mutants GagL268P or GagL322S or with (ii) N-myristylated Pr55 from the secondary mutants Gag1248myr or Gag1249myr. As controls, samples from single-infected cells (Fig. 5b) and from cells coinfected with parental Gag170 and wild-type Gag12myr were processed in parallel.

In the first type of coinfections, the sedimentation profiles of extracellular medium samples from GagL268P (or GagL322S) single-infected cell cultures were not significantly different from the pattern obtained with parental Gag170, which essentially released unassembled, soluble Gag precursor molecules (Fig. 5a). In coinfection experiments with Gag12myr and parental Gag170, 600S budded particles were found to contain both types of precursor molecules, the wild-type Pr55myr expressed by Gag12myr, and the Pr49Δmyr expressed by Gag170. The possibility that the Pr49Δmyr species was a proteolytic breakdown product from the larger Pr55myr polyprotein was excluded since Pr49Δmyr carried a polyhedrin-derived epitope tag at its N terminus (26) which reacted with anti-polyhedrin antibodies (data not shown). These results suggested that interactions between N-myristylated, full-length Gag precursor Pr55myr and non-N-myristylated, p6-deleted Gag precursor Pr49Δmyr at the plasma membrane do occur, resulting in the budding of chimeric Gag particles. Culture medium samples from cells coinfected with Gag12myr and GagL268P or GagL322S also showed the two Gag precursor species Pr55myr and Pr49Δmyr cosedimenting in the same 600S fraction (Fig. 5c). This suggested that wild-type and Sad mutant Gag precursors interacted and that both L268P and

FIG. 3. Electron micrographs of Sf9 cells singly infected with Gag10(Pr55Δmyr) (a) or coinfected with Gag10 and Gag48(L268P) (b) or Gag10 and Gag49(L322S) (c). VLP accumulate in clusters within the nucleus of Gag10-infected cells (panel a; white arrows). In coinfected cells (panels b and c), some cytoplasmic VLP are seen (arrows), often in the vicinity of electron-dense inclusions at the periphery of the nucleus (c). N, nucleus; C, cytoplasm; V, baculovirions. Bars, 1 μm.

L322S mutations expressed in the non-N-myristylated context could be rescued in *trans* by the wild-type Gag precursor to form chimeric particles released into the external medium.

In the second type of coexpression experiments, using wild-type Gag precursor-expressing Gag12myr and N-myristylated mutant Gag1248myr (or Gag1249myr), no significant difference was observed in the sedimentation profiles of extracellular Gag precursor, as compared to control Gag12myr single-infected cell cultures. This was confirmed by EM analysis showing budding particles at the plasma membrane of coinfected cells (data not shown). Since wild-type and mutant Gag precursors expressed by Gag12myr, Gag1248myr, and Gag1249myr comigrated in SDS-PAGE (in contrast to p6-deleted GagL268P and GagL322S; refer to Fig. 5), it could not be assessed whether budded particles had mixed Gag phenotypes. Nevertheless, the data suggested that the L268P and L322S mutations, expressed in the N-myristylated context, had no negative effect in *trans* over the assembly and budding of wild-type Gag particles at the plasma membrane.

DISCUSSION

Point mutants in the MA domain of the Mason-Pfizer monkey virus Gag precursor have been isolated. These mutants have been found to be altered in the transport, membrane association, or stability of intracellular viral capsids but apparently not in the primary steps of Gag precursor assembly (22, 23). In the present study, we described the isolation and characterization of two Sad point mutants of the HIV-1 Gag precursor, Gag48 and Gag49, phenotypically expressed in recombinant baculovirus-infected cells. Both mutations were mapped to the p24 domain and were found to consist of nonconservative mutations. A Leu-to-Pro substitution was found at position 268 in the Gag precursor sequence of Gag48(L268P), corresponding to residue 136 in the capsid protein p24, and a leucine-to-serine mutation was found at amino acid 322 in Gag49(L322S), i.e., residue 190 in p24. Each of the substitutions in GagL268P and GagL322S had a negative effect on the intracellular assembly of non-N-myristylated Gag precursors, resulting in a Sad phenotype. The immunoblot pattern of the Gag precursors expressed by GagL268P and GagL322S was indistinguishable from that of parental Gag170, suggesting that the Sad phenotype was not due to enhanced or premature processing of the mutant Gag precursors by cellular proteases. The defect in Gag precursor assembly observed with GagL268P and GagL322S mutants therefore resulted from structural alterations of critical regions of Gag, directly or indirectly affecting the stability or legitimacy of Gag precursor intermolecular bonds.

Some evidence supporting this hypothesis was provided by epitope analysis of the mutant Gag polyproteins, using a panel of MAb with defined reacting determinants on the Gag precursor sequence (24). Three MAb showed a significantly higher reactivity with both GagL268P and GagL322S mutants, as compared with the parental Gag precursor (data not shown). The patterns suggested that the mutations resulted in a better exposure of epitopes located near the p17-p24 cleavage site and at about 60 amino acids upstream of the p24-p9 junction. However, when Sf9 cells were doubly infected with GagL268P (or GagL322S) and PR107, an AcNPV recombinant expressing the HIV-1 protease under the control of the polyhedrin promoter (29), no significant changes were observed in the processing of the mutant Gag polyproteins in vivo, as compared to the parental Gag precursor (data not shown). This implied that the L268P and L322S mutations did not alter the accessibility of the specific cleavage sites at the p17-p24 and p24-p9 junctions. Sensitivity of mutant Gag precursors to proteases was also studied in vitro, by Glu-C proteinase and chymotrypsin followed by SDS-PAGE peptide fingerprinting, but no significant difference between the proteolytic patterns of parental and mutant Gag precursors was detected (data not shown).

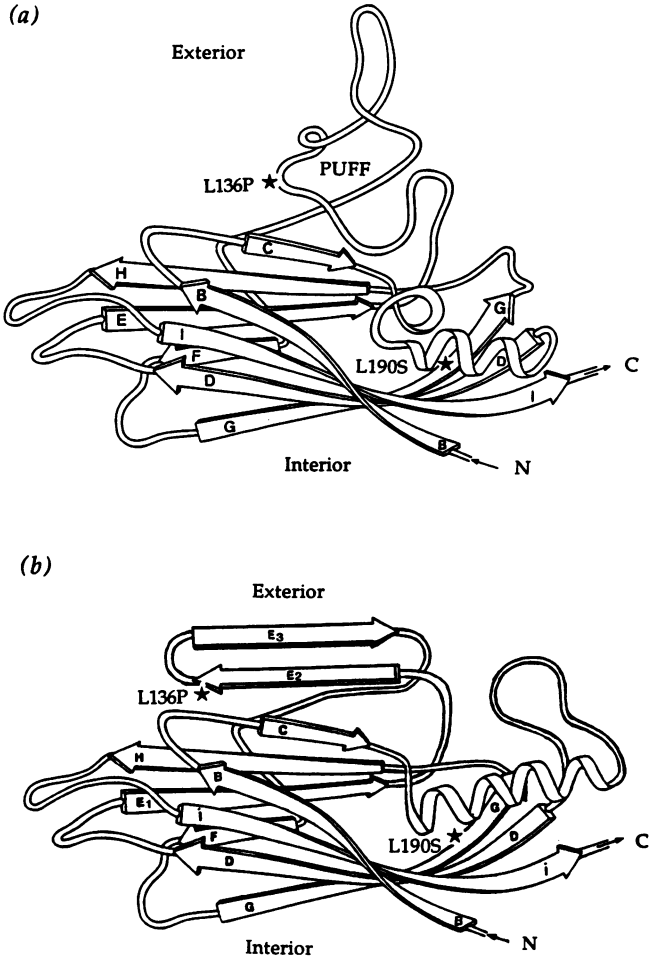

FIG. 6. Localization of the Gag48(L268P) and Gag49(L322S) mutations on the model proposed by Argos (1) (a) and (b) modified by Langedijk et al. (12) (b). The substitutions concerned the 136th and 190th residues in the p24 sequence, respectively. For convenience, the two putative additional β-strands postulated to replace the puff region in model b have been labeled E2 and E3.

The two mutated leucine in p24 are highly conserved residues in the HIV-1 *gag* gene, as shown by compiled genome sequences (16). According to structural predictions, L268P and L322S mutations are located in regions characterized by a high probability of rigidity, inaccessibility, hydrophobicity, and β-sheet conformation (24). They also present a high degree of homology among various virus species (1). Referring to two models recently proposed for p24 of HIV-1 (1, 12), the L322S mutation would be located in the distal portion of the β-strand G, involving a highly structured region (Fig. 6a and b). The L268P mutation is situated at the extremity of one of the two putative additional

β-strands proposed by Langedijk et al. (Fig. 6b). In the model of Argos (Fig. 6a) this mutated site belongs to the puff region. The deleterious effect on intracellular assembly of Gag precursor induced by the two mutations suggested that conserved polypeptide domains (1), which are essential for the proper folding of Gag polyprotein, its self-assembly, or both, were altered.

It is interesting that L268P and L322S mutations are both located in the C-terminal moiety of the p24 domain. This is in an homologous region of the Rous sarcoma virus Gag precursor, upstream of the p24-p15 junction, where the assembly domain AD3 has been recently assigned to lie (31). However, the two regions involved by L268P and L322S mutations seemed to be functionally different. (i) Some complementation effect was observed between GagL268P and GagL322S mutants in coinfection experiments, implying that one mutant domain can be rescued for intracellular assembly of Gag precursors by the sister mutant (Tables 1 and 2). (ii) When expressed in the N-myristylated, full-length Gag precursor context, the L268P and L322S mutations showed different phenotypes. L268P abolished the extracellular release of particulate and nonparticulate forms of Gag precursor, whereas L322S had little effect on the budding of Gag particles and secretion of soluble Gag precursor (Fig. 2).

Both mutations were found to exert some *trans*-dominant negative effect over the intracellular assembly of non-N-myristylated, full-length Gag precursor expressed by Gag10 (Tables 1 and 2), whereas no detectable effect was observed in *trans* over the extracellular release of N-myristylated, wild-type Gag precursor. The mechanism of *trans* dominance of GagL268P (or GagL322S) over Gag10 seemed to involve direct, but illegitimate, interactions between the two coexpressed forms of Gag precursors, as suggested by the EM observation of perinuclear inclusions (Fig. 3) and the modifications of the proteolytic cleavage pattern of Gag precursors occurring in coinfected cells (Fig. 4).

A great number of mutations will be required to determine precisely the sites and amino acid residues critical for the assembly of HIV-1 Gag precursors and the nature of their mutual bonds. Nevertheless, the two point mutations characterized in this study define two discrete assembly subsites in the carboxy-terminal moiety of the p24 domain of Gag precursor. (i) The first site, altered in the GagL268P mutant, seems to be critical for both intracellular assembly of non-N-myristylated Gag precursor and extracellular release of N-myristylated Gag precursor under particulate and nonparticulate forms. (ii) The second site, mutated in GagL322S, was apparently involved only in the intracellular assembly pathway, as the L322S mutation was rescued by the N-myristylated context. Considering *gag* as a potential target gene for viral gene therapy of HIV-1 infection (28), our data provide some clues for site-directed mutagenesis of Gag precursor assembly domains.

ACKNOWLEDGMENTS

This work was supported by the Agence Nationale de Recherche sur le SIDA (ANRS-AC14), the Direction de la Recherche et des Etudes Doctorales (DRED-1991), and the Fondation pour la Recherche Médicale. S.S.H. was the recipient of an ANRS fellowship.

We are indebted to Nicole Vidal and Gérard Cuny (ORSTOM) for help with DNA sequencing, to Jeannette Tournier for the EM processing, and to Bernard Gay for the photographic reproductions. We also thank Hanno Kolbe for providing us with purified recombinant p24, Christian Devaux for his panel of anti-Gag MAb, Monique Royer for her PR107 and PR77 recombinants, and John Wills for fruitful discussions.

REFERENCES

1. **Argos, P.** 1989. A possible homology between immunodeficiency virus p24 core protein and picornaviral VP2 coat protein: prediction of HIV p24 antigenic sites. EMBO J. **8**:779–785.
2. **Cann, A. J., and J. Karn.** 1989. Molecular virology of HIV: new insights into the virus life-cycle. AIDS **3**(Suppl. 1):S19–S34.
3. **Cleveland, D. W., S. G. Fisher, M. W. Kirshna, and U. K. Laemmli.** 1977. Peptide mapping by limited proteolysis in sodium dodecyl sulfate and analysis by gel electrophoresis. J. Biol. Chem. **252**:1102–1106.
4. **Delchambre, M., D. Gheysen, D. Thines, C. Thiriart, E. Jacobs, E. Verdin, M. Horth, A. Burny, and F. Bex.** 1989. The GAG precursor of simian immunodeficiency virus assembles into virus-like particles. EMBO J. **8**:2653–2660.
5. **Gelderblom, H. R.** 1991. Assembly and morphology of HIV: potential effect of structure on viral function. AIDS **5**:617–638.
6. **Gheysen, D., E. Jacobs, F. de Foresta, C. Thiriart, M. Francotte, D. Thines, and M. De Wilde.** 1989. Assembly and release of HIV-1 precursor Pr55gag virus-like particles from recombinant baculovirus-infected insect cells. Cell **59**:103–112.
7. **Hoshikawa, N., A. Kojima, A. Yasuda, E. Takayashiki, S. Masuko, J. Chiba, T. Sata, and T. Kurata.** 1991. Role of the *gag* and *pol* genes of human immunodeficiency virus in the morphogenesis and maturation of retrovirus-like particles expressed by recombinant vaccinia virus: an ultrastructural study. J. Gen. Virol. **72**:2509–2517.
8. **Hunkapiller, T., R. J. Kaiser, B. F. Koop, and L. Hood.** 1991. Large-scale and automated DNA sequence determination. Science **254**:59–67.
9. **Jowett, J. B. M., D. J. Hockley, M. V. Nermut, and I. M. Jones.** 1992. Distinct signals in HIV-1 Pr55 necessary for RNA binding and particle formation. J. Gen. Virol. **73**:3079–3086.
10. **Kristensen, T., H. Voss, C. Schwager, J. Stegemann, B. Sproat, and W. Ansorge.** 1988. T7 DNA polymerase in automated dideoxy sequencing. Nucleic Acids Res. **16**:3487–3496.
11. **Laemmli, U. K.** 1970. Cleavage of structural proteins during the assembly of the head of bacteriophage T4. Nature (London) **227**:680–685.
12. **Langedijk, J. P. M., J. J. Schalken, M. Tersmette, J. G. Huisman, and R. H. Meloen.** 1990. Location of epitopes on the major core protein p24 of human immunodeficiency virus. J. Gen. Virol. **71**:2609–2614.
13. **Layne, S. P., M. J. Merges, M. Dembo, J. L. Spouge, S. R. Conley, J. P. Moore, J. L. Raina, H. Renz, H. R. Gelderblom, and P. L. Nara.** 1992. Factors underlying spontaneous inactivation and susceptibility to neutralization of human immunodeficiency virus. Virology **189**:695–714.
14. **Martin, G. R., R. Warocquier, C. Cousin, J. C. D'Halluin, and P. Boulanger.** 1978. Isolation and characterization of human adenovirus type 2 temperature-sensitive mutants. J. Gen. Virol. **41**:303–314.
15. **Mervis, R. J., N. Ahmad, E. P. Lillehoj, M. G. Raum, F. H. R. Salazar, H. W. Chan, and S. Venkatesan.** 1988. The gag gene products of human immunodeficiency virus type 1: alignment within the gag open reading frame, identification of posttranslational modifications, and evidence for alternative gag precursors. J. Virol. **62**:3993–4002.
16. **Myers, G., J. A. Berzofsky, B. Kober, R. F. Smith, and G. N. Pavlakis (ed.).** Human retroviruses and AIDS 1991. A compilation and analysis of nucleic acid and amino acid sequences, May 1991, vol. 2. Theoretical Biology and Biophysics, p. 5–9. Los Alamos National Laboratory, Los Alamos, N.Mex.
17. **Novelli, A., and P. Boulanger.** 1991. Assembly of adenovirus type 2 fiber synthesized in cell-free translation system. J. Biol. Chem. **266**:9299–9303.
18. **Novelli, A., and P. Boulanger.** 1991. Deletion analysis of functional domains in baculovirus-expressed adenovirus type 2 fiber. Virology **185**:365–376.
19. **Overton, H. A., Y. Fuji, I. R. Price, and I. M. Jones.** 1989. The protease and gag gene products of the human immunodeficiency virus: authentic cleavage and post-translational modification in an insect cell expression system. Virology **170**:107–116.
20. **Overton, H. A., D. J. McMillan, S. J. Gridley, J. Brenner, S.**

Redshaw, and J. S. Mills. 1990. Effect of two novel inhibitors of the human immunodeficiency virus protease on the maturation of the HIV *gag* and *gag-pol* polyproteins. Virology **179:**508–511.

21. **Rasmussen, L., J. K. Battles, W. H. Ennis, K. Nagashima, and M. A. Gonda.** 1990. Characterization of virus-like particles produced by a recombinant baculovirus containing the gag gene of the bovine immunodeficiency-like virus. Virology **178:**435–451.
22. **Rhee, S. S., and E. Hunter.** 1990. A single amino acid substitution within the matrix protein of a type D retrovirus converts its morphogenesis to that of a type C retrovirus. Cell **63:**77–86.
23. **Rhee, S. S., and E. Hunter.** 1991. Amino acid substitutions within the matrix protein of type D retroviruses affects assembly, transport and membrane association of a capsid. EMBO J. **10:**535–546.
24. **Robert-Hebmann, V., S. Emiliani, F. Jean, M. Resnicoff, F. Traincard, and C. Devaux.** 1992. Clonal analysis of murine B-cell response to the human immunodeficiency virus type 1 (HIV-1) *gag*p17 and p25 antigens. Mol. Immunol. **29:**729–738.
25. **Royer, M., M. Cerutti, B. Gay, S. S. Hong, G. Devauchelle, and P. Boulanger.** 1991. Functional domains of HIV-1 *gag*-polyprotein expressed in baculovirus-infected cells. Virology **184:**417–422.
26. **Royer, M., S. S. Hong, B. Gay, M. Cerutti, and P. Boulanger.** 1992. Expression and extracellular release of human immunodeficiency virus type 1 Gag precursors by recombinant baculovirus-infected cells. J. Virol. **66:**3230–3235.
27. **Tatsumi, M., F. Jean, V. Robert, J. C. Chermann, and C. Devaux.** 1990. Use of monoclonal antibodies for the detection and quantitation of HIV-1 core protein p25: comparative evaluation of in vitro HIV-1 infection by immunofluorescence, antigen capture ELISA and reverse transcriptase assays. Res. Virol. **141:**649–661.
28. **Trono, D., M. B. Feinberg, and D. Baltimore.** 1989. HIV-1 gag mutants can dominantly interfere with the replication of the wild-type virus. Cell **59:**113–120.
29. **Valverde, V., P. Lemay, J. M. Masson, B. Gay, and P. Boulanger.** 1992. Autoprocessing of HIV-1 protease precursor expressed in *E. coli* from a synthetic gene. J. Gen. Virol. **73:**639–651.
30. **Wain-Hobson, S., P. Sonigo, O. Danos, S. Cole, and M. Alizon.** 1985. Nucleotide sequence of the AIDS virus, LAV. Cell **40:**9–17.
31. **Wills, J. W., and R. C. Craven.** 1991. Form, function, and use of retroviral gag proteins. AIDS **5:**639–654.